Surface wake in the random-phase approximation

F. J. García de Abajo
Departamento de Ciencias de la Computación e Inteligencia Artificial, Facultad de Informática, Universidad del País Vasco, Apartado 649, 20080 San Sebastián, Spain

P. M. Echenique
Departamento de Física de Materiales, Facultad de Química, Universidad del País Vasco, Apartado 1072, 20080 San Sebastian, Spain

(Received 11 March 1993; revised manuscript received 10 June 1993)

The scalar-electric-potential distribution set up by an ion traveling in the vicinity of a plane solid-vacuum interface, that is, the surface-wake potential, is investigated with the specular-reflection model to describe the response of the surface and with the random-phase approximation for the dielectric function of the bulk material. This permits us to address the study of the low-velocity surface wake: the static potential is found to have a dip at the position of the ion; that dip is shifted towards the direction opposite to the velocity vector for velocities smaller than the threshold of creation of plasmons ($\approx 1.3v_F$). Extensive numerical calculations are presented for an ion both inside and outside aluminum. Comparison to the results obtained with the plasmon-pole dielectric function indicates excellent agreement for velocities larger than $\approx 1.3v_F$. On the other side, the possibility of surface-wake riding is suggested, by analogy with bulk-wake riding postulated in the past. In it, the electron would be bound in the first trough of the surface-wake potential set up when the ion describes a grazing trajectory. The main feature introduced by the surface with respect to the bulk consists of allowing the use of ions of higher charge, reducing in this way the relative importance of the electron self-energy, and in addition, giving rise to larger binding energies. When the ion beam is directed along a special direction of an oriented crystal surface, the mechanism of resonant coherent excitation could provide a way for experimentally detecting this phenomenon through the emission of the bound electron with well-defined energy and around a preferential direction.

I. INTRODUCTION

We denote by "surface-wake potential" the scalar-electric-potential distribution set up by a swift charge moving with constant velocity in the vicinity of a solid surface, which, as in the case of a particle traveling in the bulk material, where one speaks about wake phenomena,[1–5] displays an oscillatory behavior for velocities well above the Fermi velocity of the medium, v_F. The (bulk) wake potential, first studied by Neufeld and Ritchie,[1] has been the subject of intense research on many occasions.[2–5] In the present work, we shall concentrate on the surface-wake potential and the possibility of electron surface-wake riding. The former includes both the formation and destruction process of the wake, when the ion enters or leaves the medium, and the situation in which the ion finds itself traveling parallel to the surface. In this latter case, the surface-wake potential is time independent in the rest frame of the particle.

Various approximations to the surface response have been proposed in the past. Lang and Kohn,[6] for instance, used the density-functional formalism[7] to calculate the image potential in the static case (this approach produces quite interesting results when it is applied to obtain the energy shift and broadening of hydrogenic states near a surface[8]). A Hamiltonian formulation of the problem, which makes use of second quantization in both surface and bulk plasma modes, has been often utilized,[9–21] though it does not include the continuum of electron-hole pair excitations. The specular-reflection model (SRM), introduced by Ritchie and Marusak[22] in the study of the surface plasmon dispersion relation, and independently discussed by Wagner,[23] incorporates the effect of plasmon dispersion and single-particle excitations in the surface response. The latter constitutes a powerful tool that is going to be followed in the present work.

In the SRM, the surface response is expressed in terms of the dielectric function of the bulk material $\varepsilon(k,\omega)$. Different approximations to $\varepsilon(k,\omega)$ have been employed to evaluate some aspects of the surface-wake potential. For example, Chan and Richmond[24] studied the image potential in a specularly reflected trajectory using the SRM and the hydrodynamic approximation[25] to $\varepsilon(k,\omega)$. Eriksson, Karlsson, and Wijewardena[26] evaluated the potential at the surface using the same model, inspired in the SRM as described by Heinrichs;[27] their results coincide with the ones obtained from the linearized Bloch hydrodynamical model, imposing as matching conditions the continuity of both the potential and its normal derivative at the surface, together with the vanishing of the induced charge outside the surface.[28] The plasmon-pole approximation to the dielectric function[29] (PLA) is expected to work well at high velocities, where plasmons make a dominant contribution to the induced potential.[30] The full random-phase approximation for the bulk dielectric function[31] (RPA) will be used here and compared with the results obtaining using the PLA. This will permit us to evaluate the surface wake potential in a wide range of velocities. Let us mention that Gumbs and Glasser[32] have recently calculated, using the RPA, the potential set up by a particle moving in vacuum, parallel with a solid surface.

0163-1829/93/48(18)/13399(9)/$06.00 ©1993 The American Physical Society

When the particle velocity exceeds the Fermi velocity of the medium, some oscillations appear in the induced potential and charge density (this motivates the name of wake), whose origin may be found in the excitation of both bulk and surface plasmons, and whose frequency equals the bulk and surface plasma frequency, respectively. This velocity behavior is similar to that exhibited by the bulk wake.[33]

The surface-wake potential must be accounted for in a number of ion-surface scattering processes, like the vicinage effect,[10] specular reflection of ions at surfaces,[34] acceleration of the convoy electron peak in grazing ion-surface collisions,[35,36] Coulomb explosion of molecular ions induced by surface interaction,[37,38] acceleration of multicharged ions due to the image potential,[39] shock electron emission,[40] secondary electron emission,[41] etc. Also, the transition energies involved in ion-induced low-energy electron emission are small, so that a good description of the low-frequency solid response, as that provided by the surface-wake potential in the RPA, becomes necessary.

In the present work, the surface wake is investigated in Sec. II for low velocities of the particle using the SRM and the RPA. The parallel and perpendicular motion cases are discussed separately.

A curious way of binding to the wake potential was postulated two decades ago by Neelavathi, Ritchie, and Brandt.[2] In it, an electron would be traveling trapped in the regions of energy minima of the oscillatory bulk wake set up by an ion moving in the volume of a solid. Those authors estimated the binding energy using a classical frequency-dependent dielectric function to represent the response of the medium. More sophisticated approximations to the dielectric function where used later,[3,4,42] including the RPA.[5,33,43] Although several attempts were made to experimentally identify these wake-riding (WR) electrons in the convoy electron emission,[44–49] no conclusive result came out, except that they must represent a very small fraction of the total emission. Posterior calculations showed that the rate of capture into WR states was very low in first-order perturbation theory, either from target atoms[50] or from the conduction band of the solid;[51] indeed, Burgdörfer, Wang, and Müller have claimed that the second-order Thomas double-scattering mechanism provides the dominant contribution of the capture probability.[52] More recently, the use of negatively charged leading ions (e.g., μ mesons or antiprotons) has been explored both theoretically[52,53] and experimentally.[54] The bound electron is located three times closer to the projectile in that case, and therefore, the capture probabilities are dramatically enhanced.[52] Besides, the absence of the cusplike structure, characteristic of the electron emission after bombardment with positive ions, makes it easier the observation of WR states. Although Monte Carlo estimates seem to indicate the presence of a broad peak in the forward emission due to WR states,[52] no experimental investigation has been successful in uniquely determining this prediction.[54]

The surface-wake potential[55] created by an ion interacting with a solid surface under grazing incidence conditions may give rise to wake binding as well. Several substantial differences with respect to the bulk tend to increase, in principle, the likelihood of experimental observation in this hypothetical kind of binding. This point will be discussed in Sec. III.

Atomic units (a.u.) will be used throughout this work, unless otherwise specified. The surface will be chosen at the plane $z=0$, with the solid in the $z<0$ region. Z_1 and $\mathbf{v}$ will denote the charge and velocity of the ion. The notation $v=|\mathbf{v}|$, $\mathbf{k}=(\mathbf{Q},k_z)$, $\mathbf{v}=(\mathbf{V},v_z)$, and $\mathbf{r}=(\mathbf{R},z)$, where $\mathbf{Q}$, $\mathbf{V}$, and $\mathbf{R}$ represent components parallel with the surface, will be adopted.

II. THE SURFACE WAKE

The SRM, used in this work to calculate the surface-wake potential, that is, the scalar electric potential setup by a swift charge point particle moving near a solid surface, receives its name from the intrinsic assumption that the electrons of the solid rebound specularly on the surface, without any sort of interference between outgoing and reflected components.[22] Its equivalence with the semiclassical infinite barrier model, in which the surface is assimilated to an infinite potential barrier, has been proved elsewhere.[56,57] In it, the independent electron wave functions obtained with the infinite barrier potential are inserted in the pair-approximation expression for the susceptibility,[56–58] and when the interference terms between incoming and outgoing components of the electron states are neglected,[56] the surface susceptibility is reduced to an expression which depends only on the bulk dielectric function.

This model has been applied to the study of the interaction of charges with plane-bounded solids, using different dielectric functions for the bulk material.[26,32,55,56,59,60] In this work, we use the full RPA expression for the bulk response[31] in order to investigate the (low) velocity behavior of the surface wake. This may be considered as an extension to the work of Mazarro, Echenique, and Ritchie[33] who calculated the bulk-wake potential within that approximation to the solid response.

A. Parallel trajectory

The case of a particle traveling parallel with the surface is analyzed here separately. The particle does not cross the surface, what means that the algebra remains simple. Let z_0 denote the z coordinate of the particle (impact parameter). The surface-wake potential in the case of an external trajectory ($z_0>0$) reads[55,59]

$$\phi_{\parallel}^{z_0>0}(\mathbf{r},t)=\frac{Z_1}{2\pi}\int\frac{d\mathbf{Q}}{Q}e^{i\mathbf{Q}\cdot\tilde{\mathbf{R}}}\times\begin{cases}\dfrac{\varepsilon_s(Q,\omega)-1}{\varepsilon_s(Q,\omega)+1}e^{-Q(z+z_0)}+e^{-Q|z-z_0|} & \text{for } z>0 \text{ (vacuum)}\\[2ex] \dfrac{2e^{-Qz_0}}{\varepsilon_s(Q,\omega)+1}\varepsilon_s(Q,z,\omega) & \text{for } z<0 \text{ (solid)}\,,\end{cases} \tag{1}$$

whereas in the case of an inner trajectory ($z_0<0$) it is

$$\phi_{\parallel}^{z_0<0}(\mathbf{r},t)=\frac{Z_1}{2\pi}\int\frac{d\mathbf{Q}}{Q}e^{i\mathbf{Q}\cdot\tilde{\mathbf{R}}}\times\begin{cases}\dfrac{2\varepsilon_s(Q,z_0,\omega)}{\varepsilon_s(Q,\omega)+1}e^{-Qz} & \text{for } z>0 \text{ (vacuum)}\\ \varepsilon_s(Q,z-z_0,\omega)+\varepsilon_s(Q,z+z_0,\omega)-\dfrac{2\varepsilon_s(Q,z_0,\omega)}{\varepsilon_s(Q,\omega)+1}\varepsilon_s(Q,z,\omega) & \text{for } z<0 \text{ (solid)}\,,\end{cases} \tag{2}$$

where $\omega=\mathbf{Q}\cdot\mathbf{V}$, $\tilde{\mathbf{R}}=\mathbf{R}-\mathbf{V}t$,

$$\varepsilon_s(Q,z,\omega)=\frac{Q}{\pi}\int\frac{dk_z}{k^2}\frac{\cos k_z z}{\varepsilon(k,\omega)}\,, \tag{3}$$

$k^2=Q^2+k_z^2$, and $\varepsilon_s(Q,\omega)=\varepsilon_s(Q,0,\omega)$ is the surface dielectric function.[61] The first term in the integral of Eq. (2) for $z<0$ coincides with the bulk-wave potential, and the last term in Eq. (1) for $z>0$ is the direct Coulomb potential.

The function (3) satisfies the following interesting property:

$$\partial_z\varepsilon_s(Q,0^{\pm},\omega)=\begin{cases}\mp Q & \text{if } \varepsilon(\infty,\omega)=1\,,\\ \dfrac{\mp Q}{\varepsilon(\omega)} & \text{if } \varepsilon(k,\omega)=\varepsilon(\omega)\,.\end{cases} \tag{4}$$

Exploiting this identity, one can show that the electric field is continuous at the surface when $\varepsilon(\infty,\omega)=1$. In other words, the matching conditions imposed in the SRM, namely, the continuity of both the potential and the normal component of the electric displacement, imply, when effects of dispersion are included, the continuity of the electric field as well. However, in a dispersionless description of the medium, where $\varepsilon(k,\omega)=\varepsilon(\omega)$, the normal electric field presents a discontinuity at the surface, related to the creation of a sheet of surface charge.[62]

The induced surface-wake potential (i.e., the surface-wake potential minus the bare Coulomb potential created by the external charge) calculated from Eqs. (1)–(3), is depicted in Figs. 1–3 for a proton moving parallel with an aluminum surface ($r_s=2.07$). The damping of electron gas motion in the solid has been introduced through the Mermin prescription,[63] taking $\gamma=0.5$ eV.[64] The velocity dependence of the induced potential at the position of the projectile is shown in Fig. 1 for different values of the impact parameter z_0 (we have defined $\lambda=\pi v_F/2\omega_s\approx 3.54$ a.u.). Using the RPA dielectric function (continuous curves), the potential varies very little with the velocity for $v<1.3v_F$. The PLA[55] (broken curves) provides similar results to those obtained using the RPA for $v>1.3v_F$. This limiting value of the velocity is such that the straight line $\omega=kv$ passes close to the point where the bulk and surface plasmon lines intersect the continuum of electron-hole pair excitations in the k-ω plane (this happens for $v=1.27$ a.u. in Al). The integration area in the k-ω plane increases linearly with v and, therefore, the potential becomes proportional to the inverse of v at larger velocities (e.g., the dotted curve for $z_0=0$, which represents the undispersive result $-\pi\omega_s/2v$). In the large z_0 limit, the potential approaches the classical result $-1/2z_0$.

Figure 2 shows the induced potential at the position of the proton as a function of the impact parameter. Again, the results obtained using the RPA (continuous curves) do no change significantly with the velocity of the ion when $v\le 1.3v_F$. The potential decreases with increasing velocities and its spatial variation is smoothed. The screening provided by the Thomas-Fermi approximation to the RPA (dotted curve for $v=0$) is larger than that derived from the RPA in the static case, especially in the solid region. This is due to the different behavior exhibited by these response functions at large momenta ($\omega=0$):$1+O(k^{-2})$ and $1+O(k^{-4})$, respectively. Besides, the agreement between the PLA (dashed curves) and the RPA dielectric functions is excellent for $v\ge 1.3v_F$.

The induced surface-wake potential is shown in Fig. 3 in the points of the trajectory, when the proton is moving to the right near an Al surface, for different impact parameters and low velocities. The potential practically reaches its bulk limit at $z_0=-\lambda/4$. A velocity behavior similar to that observed in the bulk wake[33] is seen through the series of plots: for $v=0$ the potential presents a dip at the position of the projectile; when the ion moves slowly the dip is shifted to the left; at larger velocities

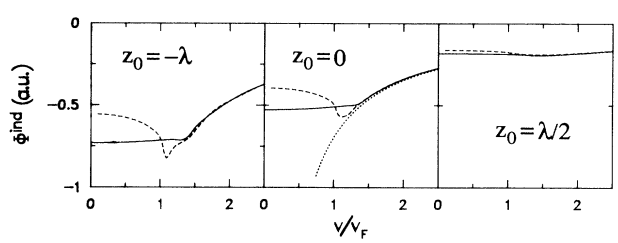

FIG. 1. Velocity dependence of the induced surface-wake potential at the position of a proton ($z=z_0$, $\mathbf{R}=\mathbf{V}t$) traveling parallel with an aluminum surface (the solid parameters have been set as $r_s=2.07$ and $\gamma=0.5$ eV (Ref. 64); the solid is contained in the $z<0$ region). The specular-reflection model (SRM), together with the RPA (continuous curves) and the plasmon-pole approximation (PLA, taken from Ref. 55; broken curves) dielectric functions, has been used to calculate the potential according to Eqs. (1)–(3). Different impact parameters have been considered (see figure, where $\lambda=\pi v_F/2\omega_s=3.54$ a.u.). The results obtained using the classical frequency-dependent response function are represented by a dotted curve for $z_0=0$.

($v > 1.3v_F$) some oscillations appear behind the particle, whose wavelengths increase with the velocity according to $2\pi v/\omega_p$, in the solid side,[1-5] and $2\pi v/\omega_s$, in the vacuum.[55] The Thomas-Fermi approximation (dotted curve) produces results that differ from those obtained by using the RPA (solid curves) for $v=0$, especially in the vicinity of the proton, where the large momentum behavior becomes important. The agreement with the results obtained using the PLA dielectric function (dashed curves) is only good at high velocities ($v > 1.3v_F$).

B. General trajectory

For an arbitrary orientation of the particle trajectory with respect to the solid surface (the origin of coordinates is taken to coincide with the point where the particle passes through the surface, and that happens when $t=0$), the scalar potential reads[55]

$$\phi(\mathbf{r},t)=\frac{1}{(2\pi)^3}\int d\mathbf{Q}\int_{-\infty}^{\infty} d\omega e^{i(\mathbf{Q}\cdot\mathbf{R}-\omega t)}\phi(\mathbf{Q},z,\omega)\ , \tag{5}$$

where

$$\phi(\mathbf{Q},z,\omega)=\frac{4\pi Z_1}{\tilde{k}^2|v_z|}\times\begin{cases}\Delta e^{-Q|z|}+e^{i\tilde{\omega}z/v_z} & \text{for } z>0 \text{ (vacuum)}\ ,\\ \zeta(\mathbf{Q},z,\omega)-\Delta\varepsilon_s(Q,z,\omega)+\dfrac{e^{i\tilde{\omega}z/v_z}}{\varepsilon(\tilde{k},\omega)} & \text{for } z<0 \text{ (solid)}\ ,\end{cases} \tag{6}$$

$\tilde{\omega}=\omega-\mathbf{Q}\cdot\mathbf{V}$, $\tilde{k}^2=Q^2+\tilde{\omega}^2/v_z^2$, and

$$\Delta=\frac{[1/\varepsilon(\tilde{k},\omega)-1]+\zeta(\mathbf{Q},0,\omega)}{\varepsilon_s(Q,\omega)+1}\ . \tag{7}$$

In these expressions, we have made use of the function

$$\zeta(\mathbf{Q},z,\omega)=i\sin\left[\frac{\tilde{\omega}|z|}{v_z}\right]\left[\frac{1}{\varepsilon(\tilde{k},\omega)}-1\right]+\frac{i\tilde{\omega}}{\pi v_z}\int dk_z\cos k_z z\left[\frac{1}{\varepsilon(k,\omega)}-1\right]P\frac{1}{k_z^2-(\tilde{\omega}/v_z)^2}\ , \tag{8}$$

where P stands for the Cauchy's principal value. Notice that $\zeta(\mathbf{Q},z,\omega)$ vanishes if $\varepsilon(k,\omega)=\varepsilon(\omega)$.

As in the parallel case, using Eq. (4) and also

$$\partial_z\zeta(\mathbf{Q},0^{\pm},\omega)=\begin{cases}\pm\dfrac{i\tilde{\omega}}{v_z}\left[\dfrac{1}{\varepsilon(\tilde{k},\omega)}-1\right] & \text{if } \varepsilon(\infty,\omega)=1\ ,\\ 0 \quad \text{if } \varepsilon(k,\omega)=\varepsilon(\omega)\ ,\end{cases}$$

one can show that the electric field is continuous everywhere if $\varepsilon(\infty,\omega)=1$.

The induced potential at the position of the particle, when this is in the vacuum side, varies more rapidly with the distance to the surface in an outgoing trajectory (i.e., for positive values of v_z) than in the incoming case, as shown in Fig. 4 for a proton moving perpendicularly to an aluminum surface. Comparison between the results obtained using the RPA (continuous curves) and the PLA (dashed curves) dielectric functions indicates an excellent agreement in the incoming trajectories. The potential converges to the classical induced potential, $-1/2z$ (dotted curves), for large z.

The potential at the position of a proton, when it is at the surface, is represented in Fig. 5 using the SRM, together with the RPA (continuous curve) and the PLA (dashed curve). The result derived from the classical frequency-dependent dielectric function,[65] $-\pi\omega_s/2|v|$, is included as well for the sake of comparison (dotted curve). Once more, the agreement between the results

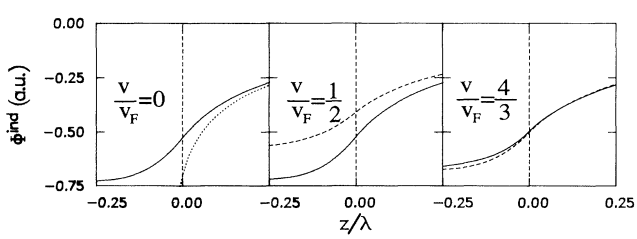

FIG. 2. Impact parameter dependence of the induced surface-wake potential at the position of a proton, moving under the conditions stated in Fig. 1, for different velocities of the projectile. Several dielectric functions are used to describe the response of the bulk material: RPA (continuous curves), PLA (broken curves), and Thomas-Fermi approximation to the RPA (dotted curve for $v=0$).

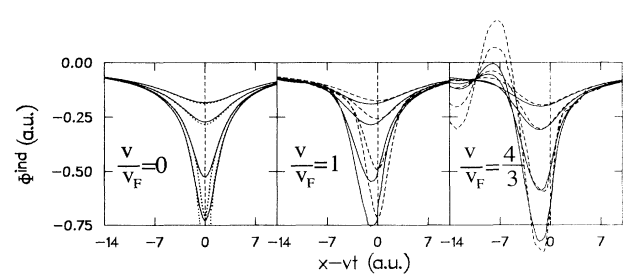

FIG. 3. Induced surface-wake potential in the points of the trajectory of a proton ($y=0$, $z=z_0$), moving along the x direction under the same conditions as in Fig. 1, towards the right, for various particle velocities. Different impact parameters are considered for each velocity: $z_0=-\lambda/4$, 0, $\lambda/4$, and $\lambda/2$ (from bottom to top). The bulk dielectric function has been taken to be the RPA (continuous curves), the PLA (broken curves), and the Thomas-Fermi approximation (dotted curves for $v=0$).

obtained using the RPA and the PLA dielectric functions is good only for $|v| > 1.3v_F$.

Figure 6 represents the induced surface-wake potential at the surface ($z=0$), set up by a proton traveling perpendicularly to an aluminum surface, for different positions of the particle. The potential decreases with R, the distance to the trajectory. The smaller vt, the stronger the induced potential in the incoming trajectories. However, that is no longer true in the outgoing case.

C. Charge density

The induced charge-density characteristic of the surface wake can be obtained by inserting Eqs. (1), (2), (5), and (6) into Poisson's equation. It vanishes at the vacuum in the SRM. Moreover, when the bulk medium is described by a response with dispersion such that $\varepsilon(\infty,\omega)=1$, the electric field is continuous everywhere, and the induced charge density does not have any singularity.[62] Let us focus on the parallel trajectory.

By analogy to what happens in the undispersive case, one would expect that the induced charge be concentrated near the surface when the particle is traveling outside the material, and in the neighborhood of both the surface and the external charge, when the latter is moving in the solid. After integrating over the x-y plane, one obtains ($z<0$)

$$\rho_z(z)=\int d\mathbf{R}\,\rho(\mathbf{r},t)=\begin{cases}\rho_z^0(z), & z_0>0 \text{ (external trajectory)},\\ \frac{1}{2}[\rho_z^0(z+z_0)+\rho_z^0(z-z_0)], & z_0<0 \text{ (inner trajectory)},\end{cases}$$

where the integrated charge density for an external trajectory, independent of both the velocity and the impact parameter, reads

$$\rho_z^0(z)=\frac{2Z_1}{\pi}\int_0^\infty dq\,\cos(qz)\left[\frac{1}{\varepsilon(q,0)}-1\right]. \tag{9}$$

Figure 7 shows the results obtained from Eq. (9) using the RPA. The integral of this quantity,

$$\rho_z^i(z)=\int_z^0 dz'\rho_z^0(z'), \tag{10}$$

also plotted in the figure, illustrates that most of the induced charge is closer to the surface than $\lambda/2=1.77$ a.u. in the case of an external trajectory.

The distribution of induced charge density in the plane of the surface can be analyzed by looking at the integral in the perpendicular direction. In the case of an external trajectory, one finds

$$\bar{\rho}(\mathbf{R},t)=\int_{-\infty}^0 dz\,\rho(\mathbf{r},t)$$
$$=\frac{Z_1}{(2\pi)^2}\int d\mathbf{Q}\,\frac{e^{i\mathbf{Q}\cdot\tilde{\mathbf{R}}-Qz_0}}{\varepsilon_s(Q,\omega)+1}\left[\frac{1}{\varepsilon(Q,\omega)}-1\right]$$
$$(z_0>0), \tag{11}$$

where $\omega=\mathbf{Q}\cdot\mathbf{V}$. Figure 8 shows $\bar{\rho}(\mathbf{R},t)$ along the projection of the trajectory on the surface for different velocities and impact parameters (the particle is traveling from left to right). The RPA dielectric function has been used, together with the Mermin prescription mentioned above.

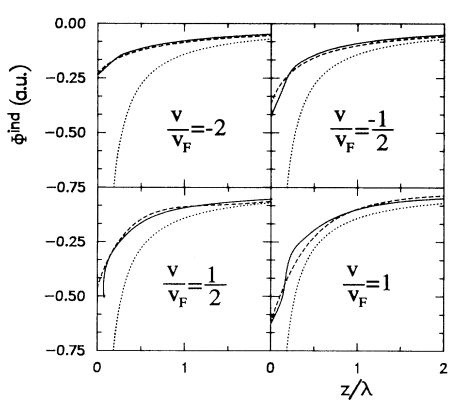

FIG. 4. Induced surface-wake potential at the position of a proton ($\mathbf{r}=\mathbf{v}t$) traveling perpendicularly to an aluminum surface for different velocities of the particle, while this is in the vacuum side. The potential has been calculated according to Eqs. (5)–(8). Continuous and broken curves stand for the results obtained by using the RPA and the PLA bulk dielectric functions, respectively. Dotted curves represent the classical induced potential in the vacuum side, $-1/2z$. Negative (positive) velocities stand for incoming (outgoing) trajectories.

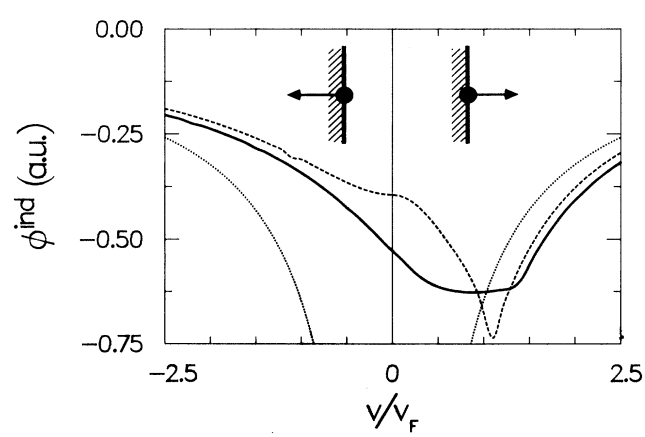

FIG. 5. Velocity dependence of the induced surface-wake potential at the position of a proton traveling perpendicularly to an aluminum surface, when the projectile is at the surface ($\mathbf{r}=\mathbf{v}t=0$). Continuous and broken curves represent the results obtained from the RPA and the PLA dielectric functions, respectively. The dotted curve stands for the results obtained from the frequency-dependent classical dielectric function (Ref. 65), $-\pi\omega_s/2|v|$.

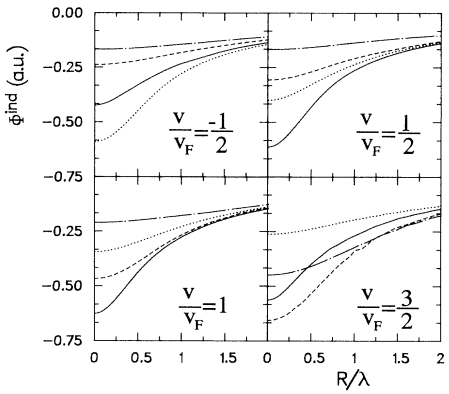

FIG. 6. Induced surface-wake potential in the plane of the surface ($z=0$), set up by a proton moving perpendicualrly to an Al-vacuum interfae for various velocities. Different times have been considered: $vt=-\lambda/2$, 0, $\lambda/2$, and λ (dotted, continuous, dashed, and dashed-dotted curves, respectively). R indicates the distance to the trajectory.

The main features observed in the induced potential are reproduced in the charge density: a dip for $v=0$, which shifts to the left as the velocity increases, and some oscillations showing up at higher velocities. The smaller $|z_0|$ the deeper the dip. Since the total induced charge must equal minus the external charge, one concludes that the former is more concentrated in the neighborhood of $\tilde{\mathbf{R}}=\mathbf{0}$ when the particle is traveling closer to the surface.

III. SURFACE-WAKE RIDING ELECTRONS

In this section, we shall focus on the possibility that an electron state can be defined in the regions of electron energy minima of the oscillatory surface wake when the external ion moves parallel with the surface. There are several differences, with respect to the case in which the

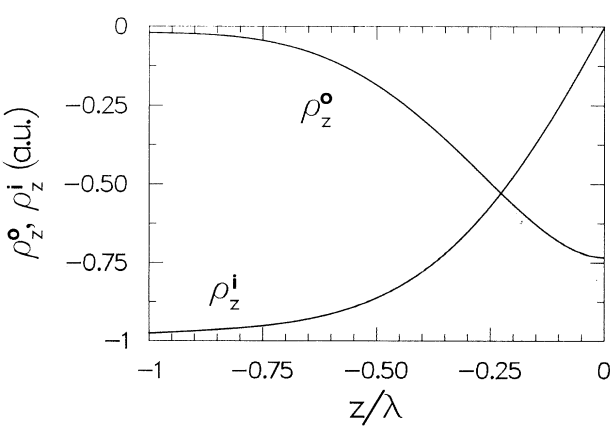

FIG. 7. Induced charge density integrated in the directions of the surface, ρ_z^0, according to Eq. (9). The RPA dielectric function has been used. The ion is taken to be a proton moving parallel with an aluminum surface, outside the mateial ($z_0>0$). The integral of ρ_z^0 in the z direction, ρ_z^i [Eq. (10)], is also shown in the figure.

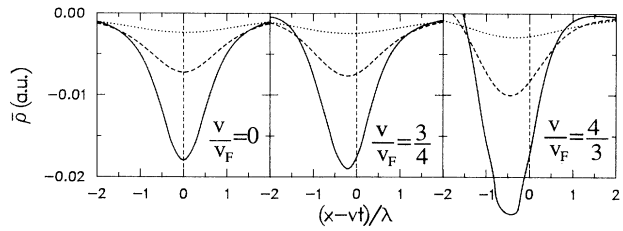

FIG. 8. Induced charge density set up by a proton moving in vacuum parallel with an aluminum surface, integrated in the direction normal to the surface, as a function of the distance measured along the trajectory, according to Eq. (11), for different velocities and impact parameters: $z_0=\lambda/2$, λ, and 2λ (continuous, dashed, and dotted curves, respectively). The proton is moving from left to right.

wake binding occurs in the bulk,[2] which tend to make the detection of this phenomenon more plausible in principle.

(i) Heavy ions can remain stripped more easily in the surface than in the bulk. Hence, leading ions of higher charge could be used, which means that the wake binding energies would be larger. In addition, the self-wake and the quantum fluctuations would lose relative importance.

(ii) The interaction with the lattice, usually argued as a mechanism that could shorten the lifetime of the WR states to the point of making them undetectable, could be exploited if the ion travels parallel with a special direction of a crystal surface. More precisely, the bound electron could undergo a resonant-coherent excitation (like in the Okorokov effect,[66,67] which takes place in the bulk) and emerge with a well-defined direction and energy.[68] When negatively charged projectiles are used, there is no other possibility of binding except for the WR states, which would remain as the only source for such a resonant process.

(iii) The total probability of capture into *WR* states and subsequent loss to the continuum of the vacuum is enhanced by the larger ion-surface interaction times.

It should be stressed that the electron-gas density decreases very rapidly with the distance to the surface; this will make the probability of capture very small, except in the turning point of the trajectory, where the density takes nearly the same value as in the bulk. The same argument applies to capture from inner shells of target atoms. Besides, the wavelength of the wake oscillations is a factor of $\sqrt{2}$ larger in the surface; thus, the bound electron would be closer in the bulk-wake riding.

Let us now present a brief estimation of the binding energies obtained for this hypothetical surface-wake riding. We will work in the rest frame of the projectile. Figure 9 illustrates the surface-wake potential, $\phi(\mathbf{r})$, set up by a charged particle traveling in the jellium edge ($z_0=0$), calculated according to Eq. (1) with the PLA dielectric function (we have defined $\lambda_s=2\pi v/\omega_s$). The electron potential energy near one of its minima can be approximated by the expression

$$V(\mathbf{r})=-\phi(\mathbf{r})\approx V_0+\frac{a^2}{2}(\tilde{x}-\tilde{x}_0)^2+\frac{b^2}{2}y^2+c\,|z-z_s|\ , \tag{12}$$

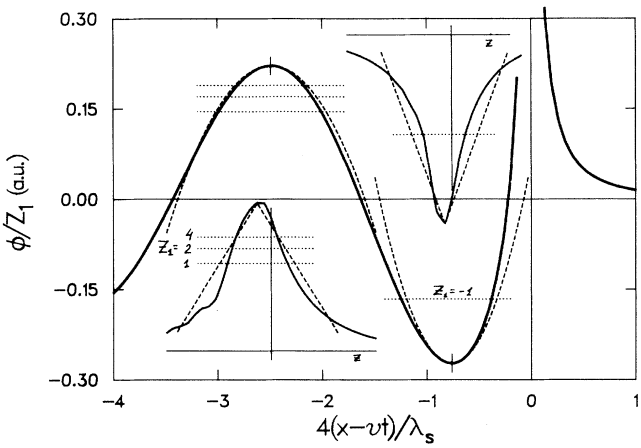

FIG. 9. Surface-wake potential in the points of the trajectory followed by a charge travelling parallel with an aluminum surface, in the jellium edge ($z_0=0$), with velocity $v=5$ a.u. The specular-reflection model (Ref. 22), together with the plasmon-pole dielectric function (Ref. 29), has been used to describe the response of the medium. We have defined $\lambda_s=2\pi v/\omega_s$. The potential is also plotted in the insets for $y=0$ along the z direction at the position of the minimum of electron potential energy ($x-vt\approx-\lambda_s/4$ for negative projectiles, and $\approx-3\lambda_s/4$ for positive ones). The dashed curves correspond to the approximation of Eq. (12). The binding energies are represented by horizontal dotted lines, which correspond to the quantity $-E_0/Z_1$. Several values of Z_1 are considered in the case of positively charged leading projectiles: $Z_1=1$, 2, and 4 (the ratio $-E_0/Z_1$ increases with Z_1).

where z_s is the z coordinate at the minimum, $\tilde{x}=x-vt$, and $\tilde{x}_0$ is its distance to the projectile [the dashed curves in Fig. 9 show this approximation as compared with the full calculation of Eq. (1)]. Notice that the first minimum in the electron potential energy is located at a distance $\approx\lambda_s/4$ behind the projectile in the case of negatively charged leading ions, and $\approx 3\lambda_s/4$ for positive ones. Then, the ground state of an electron bound in such a potential trough is of Gaussian type in the x and y directions, and an Airy function in the z direction; its energy is given by

$$E_0=V_0+(a+b)/2-(c^2/2)^{1/3}\alpha_0 , \tag{13}$$

where $\alpha_0\approx-1.019$ is the first zero of the derivative of the Airy function. The wake binding energies obtained from Eq. (13) are represented in Fig. 9 by dotted horizontal bars (in fact we have shown $-E_0/Z_1$). The ratio between the latter and the energy of the 1s state of the ion of charge Z_1, viz., $-2E_0/Z_1^2$, varies from 0.05 to 0.2 for $v=2.5-7$ a.u. and $Z_1=1-6$.

Table I shows the values of the wake binding energies obtained for different velocities and projectile charges. These values correspond to trailing probes traveling in the jellium edge ($z_0=0$). Larger binding energies are expected when the projectiles move deeper inside the solid (see the figures in parentheses for the bulk-wake riding). The values shown in the table have been obtained using the PLA dielectric function. We have checked that the same figures are obtained using the RPA in this range of velocities, as one would expect from the analysis of the surface wake carried out in the previous section. However, for lower velocities one observes appreciable differences.[43]

IV. SUMMARY

The surface-wake potential, set up by a swift charged point particle moving with constant velocity along a straight line in the vicinity of a flat solid surface, has been analyzed in the range of low velocities by using the specular-reflection model[22,23,27,56] (SRM) to describe the surface response and the RPA for the dielectric function of the bulk material. As in the bulk wake,[33] the potential distribution does not change significantly for particle velocities below the threshold of creation of plasmons ($\approx 1.3v_F$ in aluminum): a symmetric distribution of potential and charge density is observed in the static case, characterized by a dip at the position of the particle; in a trajectory parallel with the surface, the dip is shifted towards the points behind the projectile. For velocities larger than the mentioned threshold, the potential displays oscillations of frequencies ω_s (mainly in the vacuum) and ω_p (in the solid).

The potential and the electric displacement are imposed to be continuous at the surface in the SRM. Furthermore, one has that the electric field is also continuous if the bulk dielectric function goes to 1 in the large momentum limit. However, when a local dielectric function is used, the electric field presents a discontinuity at the surface, connected with the existence of a surface charge sheet. When dispersion is accounted for, the latter is mainly located within the first angstrom below the surface.

TABLE I. Wake binding energies (in eV) for different velocities and ion charges under the same conditions as in Fig. 1. The values in parenthesis correspond to the case in which the leading ion moves fully inside the bulk material. The plasmon-pole approximation[29] has been used in both cases (via the specular-reflection model[22] in the surface). The same figures are obtained within the RPA in this range of velocities.

v (a.u.)	$Z_1=-1$	$Z_1=1$	$Z_1=2$	$Z_1=4$	$Z_1=6$
2	(−1.0)	(−2.1)	−3.4	−12.1	−21.9
3	−0.6 (−3.4)	−1.7 (−4.0)	−6.0	−15.9	−26.6
4	−1.6 (−4.0)	−2.4 (−4.5)	−6.7	−16.5	−26.8
6	−2.1 (−3.9)	−2.5 (−4.3)	−6.5	−15.3	−24.3
8	−2.0 (−3.5)	−2.5 (−4.1)	−6.1	−13.9	−22.0

Using the SRM and the RPA requires an extensive investment of numerical processing, which can be softened for particle velocities larger than $\approx 2v_F$ if one replaces the RPA by the plasmon-pole approximation.[55] An excellent numerical agreement between both approximations is observed for velocities above that limit. The explanation may be found in the dominant role played by plasmons when evaluating the response of the medium to calculate the induced potential at relatively large velocities.

Finally, we have discussed the possibility of surface-wake riding, where the probe is considered to interact with the surface under grazing incidence conditions. This situation would permit to use highly charged ions, which would be neutralized in the bulk. In this way, larger binding energies would be obtained, so that the self-interaction of the electron would not play a relevant role. Also, the mechanism of resonant-coherent electron emission[68] could help to detect these states.

ACKNOWLEDGMENTS

The authors gratefully acknowledge help and support by the Departamento de Educación del Gobierno Vasco, Gipuzkoako Foru Aldundia, and the Spanish Comisión Asesora Científica y Técnica (CAICYT).

[1]J. Neufeld and R. H. Ritchie, Phys. Rev. **98**, 1632 (1955); **99**, 1125 (1955).

[2]V. N. Neelavathi, R. H. Ritchie, and W. Brandt, Phys. Rev. Lett. **33**, 302 (1974); **33**, 670(E) (1974); **34**, 560(E) (1975).

[3]R. H. Ritchie, W. Brandt, and P. M. Echenique, Phys. Rev. B **14**, 4808 (1976).

[4]P. M. Echenique, R. H. Ritchie, and W. Brandt, Phys. Rev. B **20**, 2567 (1979); J. C. Ashley and P. M. Echenique, *ibid.* **31**, 4655 (1985); **35**, 8701 (1987).

[5]P. M. Echenique, F. Flores, and R. H. Ritchie, in *Solid State Physics: Advances in Research and Applications,* edited by H. Ehrenreich and D. Turnbull (Academic, New York, 1990), Vol. **43**, p. 229.

[6]N. D. Lang and W. Kohn, Phys. Rev. B **7**, 3541 (1973).

[7]P. Hohenberg and W. Kohn, Phys. Rev. **136**, B864 (1964); W. Kohn and L. J. Sham, *ibid.* **140**, A1133 (1965).

[8]P. Nordlander and J. C. Tully, Phys. Rev. Lett. **61**, 990 (1988); Phys. Rev. B **42**, 5564 (1990).

[9]P. M. Echenique, R. H. Ritchie, N. Barberán, and J. C. Inkson, Phys. Rev. B **23**, 6486 (1981).

[10]Y. H. Ohtsuki, T. O'hori, and R. Kawai, Nucl. Instrum. Methods **194**, 35 (1982); T. O'hori and Y. H. Ohtsuki, Phys. Rev. B **27**, 3418 (1983).

[11]M. Šunjić, G. Toulouse, and A. A. Lucas, Solid State Commun. **11**, 1629 (1972).

[12]R. Ray and G. D. Mahan, Phys. Lett. **42A**, 301 (1972).

[13]J. R. Manson and R. H. Ritchie, Phys. Rev. B **24**, 4867 (1981).

[14]A. A. Lucas, Phys. Rev. B **4**, 2939 (1971).

[15]F. Sols and R. H. Ritchie, Surf. Sci. **194**, 275 (1988).

[16]B. Gumhalter and D. M. Newns, Surf. Sci. **50**, 465 (1975).

[17]A. G. Eguiluz, Solid State Commun. **33**, 21 (1980).

[18]J. W. Wu and G. D. Mahan, Phys. Rev. B **28**, 4839 (1983).

[19]J. Mahanty, K. N. Pathak, and V. V. Paranjape, Solid State Commun. **54**, 649 (1985).

[20]R. Kawai, N. Itoh, and Y. H. Ohtsuki, Surf. Sci. **114**, 137 (1982).

[21]T. Iitaka and Y. H. Ohtsuki, Surf. Sci. **213**, 187 (1989).

[22]R. H. Ritchie and A. L. Marusak, Surf. Sci. **4**, 234 (1966).

[23]D. Wagner, Z. Naturforsch. Teil A **21**, 634 (1966).

[24]D. Chan and P. Richmond, J. Phys. C **9**, 163 (1976).

[25]F. Bloch, Z. Phys. **81**, 363 (1933); Helv. Phys. Acta **7**, 385 (1934).

[26]H. G. Eriksson, B. R. Karlsson, and K. A. I. L. Wijewardena, Phys. Rev. B **31**, 843 (1985).

[27]J. Heinrichs, Phys. Rev. B **8**, 1346 (1973).

[28]R. H. Ritchie, Ph.D. thesis, University of Tennessee, 1959 (unpublished). In this thesis, the potential at the surface is derived using the hydrodynamical model.

[29]B. I. Lundqvist, Phys. Kondens. Mater. **6**, 206 (1967); Phys. Status Solidi **32**, 273 (1969).

[30]At high velocities, the response function is evaluated in a vast region of the k-ω plane, and the plasmon peak dominates in the induced potential. In this sense, the bulk solid response can be characterized by a plasmon peak, with dispersion such that it follows the single-particle-excitation energies in the large k limit. This is the PLA.

[31]J. Lindhard, Dan. Mat. Fys. Medd. **28**, no. 8 (1954).

[32]G. Gumbs and M. L. Glasser, Phys. Rev. B **37**, 1391 (1988).

[33]A. Mazarro, P. M. Echenique, and R. H. Ritchie, Phys. Rev. B **27**, 4117 (1983).

[34]K. Kimura, M. Hasegawa, Y. Fujii, M. Suzuki, Y. Susuki, and M. Mannami, Nucl. Instrum. Methods B **33**, 358 (1988).

[35]T. Iitaka, Y. H. Ohtsuki, A. Koyama, and H. Ishikawa, Phys. Rev. Lett. **65**, 3160 (1990); A. Koyama, Y. Sasa, H. Ishikawa, A. Misu, K. Ishii, T. Iitaka, Y. H. Ohtsuki, and M. Uda, *ibid.* **65**, 3156 (1990).

[36]K. Kimura, M. Tsuji, and Michi-hiko Mannami, Phys. Rev. A **46**, 2618 (1992).

[37]Y. Susuki, H. Mukai, K. Kimura, and M. Mannami, Nucl. Instrum. Methods B **48**, 347 (1990).

[38]H. Winter, J. C. Poizat, and J. Remillieux, Nucl. Instrum. Methods B **67**, 345 (1992).

[39]H. Winter, Europhys. Lett. **18**, 207 (1992).

[40]M. Burkhard *et al.*, Phys. Rev. Lett. **58**, 1773 (1987).

[41]See, for instance, K. O. Groeneveld, R. Maier, and H. Rothard, Nuevo Cimento **12**, 843 (1990) and references therein.

[42]M. H. Day, Phys. Rev. B **12**, 514 (1975); M. Day and M. Ebel, Phys. Rev. B **19**, 3434 (1979).

[43]P. M. Echenique and R. H. Ritchie, Phys. Rev. B **21**, 5854 (1980).

[44]W. Brandt and R. H. Ritchie, Phys. Lett. **62A**, 374 (1977).

[45]A. Gladieux and A. Chateau-Thierry, Phys. Rev. Lett. **47**, 786 (1981).

[46]W. Meckbach, N. Arista, and W. Brandt, Phys. Lett. **65A**, 113 (1978).

[47]R. Laubert, I. A. Sellin, C. R. Vane, M. Suter, S. B. Elston, G. D. Alton, and R. S. Thoe, Phys. Rev. Lett. **41**, 712 (1978).

[48]M. W. Lucas, W. Steckelmacher, J. Macek, and P. E. Potter, J. Phys. B **13**, 4833 (1980).

[49]N. Oda, Y. Yamazaki, and Y. Yamaguchi, J. Phys. Soc. Jpn. **53**, 3250 (1984); Y. Yamazaki and N. Oda, Nucl. Instrum.

Methods B **10/11**, 161 (1985).
[50]Y. Yamazaki and N. Oda, Nucl. Insrum. Methods **194**, 415 (1982).
[51]P. M. Echenique and R. H. Ritchie, Phys. Lett. **111A**, 310 (1985).
[52]J. Burgdörfer, J. Wang, and J. Müller, Phys. Rev. Lett. **62**, 1599 (1989).
[53]A. Rivacoba and P. M. Echenique, Phys. Rev. B **36**, 2277 (1987).
[54]Y. Yamazaki, Nucl. Instrum. Methods B **48**, 97 (1990).
[55]F. J. García de Abajo and P. M. Echenique, Phys. Rev. B **46**, 2663 (1992).
[56]F. García-Moliner and F. Flores, *Introduction to the Theory of Solid Surfaces* (Cambridge University Press, Cambridge, England, 1979).
[57]Z. Penzar and M. Šunjić, Phys. Scr. **30**, 453 (1984).
[58]L. Hedin and S. Lundqvist, Solid State Phys. **23**, 1 (1969).
[59]R. Núñez, P. M. Echenique, and R. H. Ritchie, J. Phys. C **13**, 4229 (1980); P. M. Echenique, Philos. Mag. B **52**, L9 (1985); N. Zabala and P. M. Echenique, Ultramicroscopy **32**, 327 (1990).
[60]F. Flores and F. García-Moliner, J. Phys. C **12**, 907 (1979).
[61]D. M. Newns, Phys. Rev. B **1**, 3304 (1970).
[62]K. L. Kliewer and R. Fuchs, Phys. Rev. **172**, 607 (1968); K. L. Kliewer, Phys. Rev. B **14**, 1412 (1976).
[63]N. D. Mermin, Phys. Rev. B **1**, 2362 (1970).
[64]The width of the bulk plasmons for Al is given in K. J. Krane, J. Phys. F **10**, 2133 (1978) as a function of the momentum. For simplicity, we have adopted the value for $k=0$, since our results will not depend appreciably on this choice.
[65]J. Harris and R. O. Jones, J. Phys. C **6**, 3585 (1973); D. Chan and P. Richmond, Surf. Sci. **39**, 437 (1973).
[66]V. V. Okorokov, D. L. Tolchenkov, I. S. Khizhnyakov, Yu. N. Cheblukov, Y. Y. Lapitski, G. A. Iferov, and Yu. N. Zhukova, Pis'ma Zh. Eksp. Teor. Fiz. **16**, 588 (1972) [JETP Lett. **16**, 415 (1972)]; Phys. Lett. **43A**, 485 (1973).
[67]Y. H. Ohtsuki, *Charged Beam Interaction With Solids* (Taylor & Francis, London, 1983).
[68]F. J. García de Abajo, V. H. Ponce, and P. M. Echenique, Phys. Rev. Lett. **69**, 2364 (1992).